PRECISION MAGNETICALLY SUSPENDED XY STAGE

Alexander Kuzin
Moscow Aviation Technological Institute, Moscow, Russia

ABSTRACT
The objective of these research efforts is to analyze, design, construct, and test a precision magnetically suspended motion control stage, allowing linear travel of 50 mm in two linear directions X and Y. The proposed stage has applications in such areas as semiconductor manufacturing and biotechnology experiments. The structure of the stage, developed equations of actuator forces and some aspects of the stage optimal design are presented.

INTRODUCTION
There are many potential applications where precision motion control is required. Semiconductor manufacturing and biotechnology experiments are some of them. There is considerable progress in the area of conventional precision motion control systems using mechanical bearings for support of moving objects. The common problem of conventional systems that they cannot operate without maintenance in super-clean and vacuum environments. They generate dust and evaporation that can be troubling for super-clean and vacuum processing and experiments.

Magnetic bearings represent a promising approach for achieving precision positioning of a moving object without mechanical contact and environment contamination.

Some of precision magnetically suspended systems have already been developed [1,2].

The objective of these research efforts is to analyze, design, construct, and test a precision magnetically suspended motion control stage, allowing linear travel of 50 mm in two linear directions X and Y.

ILLUSTRATIVE DESIGN
In one possible design, the platen is suspended by a symmetric arrangement of four electromagnetic actuators M1-M4 (Fig.1). The actuators are mounted in the machine frame and act to attract the ferromagnetic platen. The capacitance probes C1, C2 and C3 provide measurement one linear Z and two angular coordinates γ and ψ of the platen.

The structure and operating principles of electromagnetic actuators is very similar to structure and operation of conventional linear stepping motors. The actuator consists of a laminated silicon steel core with four toothed poles, permanent magnet and four coils that are wound around the toothed poles (Fig. 2). The attractive and propulsive forces are controlled by superposition of magnetic flux generated by the coils onto the bias magnetic flux of the permanent magnet. The permanent magnet provides 80% of suspended mass balancing against gravity and improves the power efficiency of the actuator. This is highly suited for precision positioning tasks where power dissipation must be minimized to reduce thermal expansion effects. To provide the levitation of the platen the gaps between the actuators and platen are controlled by controlling the magneto motive forces of the actuator coils according to the gap sensor signals. The coils A1 and A2 (B1 and B2) are

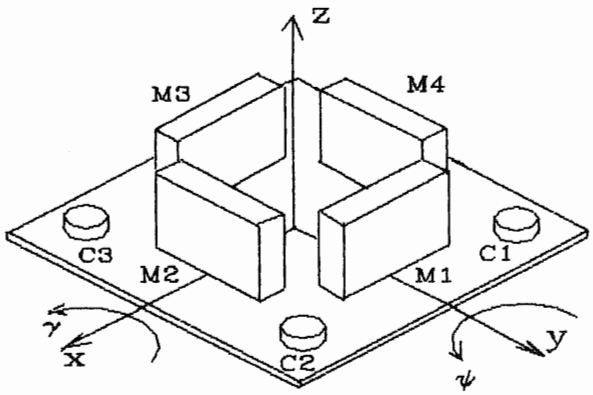

FIGURE 1: Schematical System Design

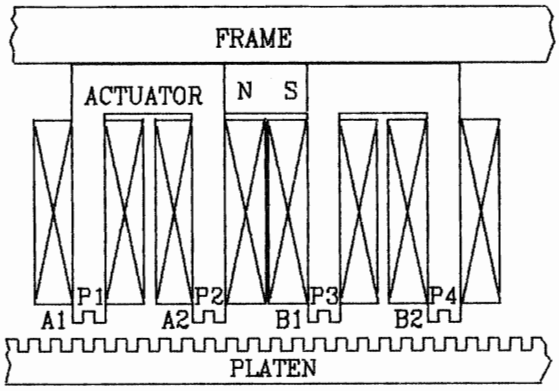

FIGURE 2: Structure of Actuator

connected in parallel. To provide the lateral movement of the platen the mini-step drive magneto motive forces are applied to coils A1, A2, B1, B2 in such a way that when the magnetic flux of one coil (A1 or B1) has the direction as bias magnetic flux, the magnetic flux of the other coil (A2 or B2) has the opposite to bias flux direction.

The platen surface under the each actuator has toothed structure of such area that provides the linear platen travel of 50 mm in two linear directions X and Y. If to define the one period of platen tooth as 2π radians, then the phase relations between the toothed poles of the actuator and platen can be expressed as following. The phase shift of P1 equal to 0 radians when teeth of toothed pole P1 are in phase with those ones of platen. In this case the phase shift of P2 pole equals to π radians. The phase shift of P3 pole equals to $-\pi/2$ radians and phase shift of pole P4 equals to $\pi/2$ radians.

The location of the actuators on the frame and the elimination of the power supply wiring to the moving platen was chosen in this design. The actuators' location on the moving platen may be preferable for some other applications.

ACTUATOR MODEL AND FORCES

An actuator design combining permanent magnet and electromagnet has the advantages of compact size, high efficiency and low heat generation. The mathematical model of actuator can be represented by the reluctance model that allows us to derive the equations for attractive and propulsive forces. Figure 3 shows the corresponding equivalent circuit of actuator, where *Um* is the magneto motive force (MMF) of permanent magnet (PM), *Uai, Ubi* are the MMFs of the coils, *Rmi* is the magnetic reluctance of the air gap under the corresponding pole; *Gmi* is the magnetic conductance (inverse to reluctance value); *Rm* is reluctance of the permanent magnet. In our analysis we suppose that effect of iron saturation is negligible and there are no leakage fluxes. Magnetic reluctance of the iron core is negligible in comparison with that one of PM and air gap. We assume that magnetic conductances of the air gaps can be represented by the following equations

$$\begin{aligned} Gm_1 &= G_0 + G\cos\varphi \\ Gm_2 &= G_0 - G\cos\varphi \\ Gm_3 &= G_0 + G\sin\varphi \\ Gm_4 &= G_0 - G\sin\varphi \end{aligned} \tag{1}$$

$$\begin{aligned} G_o &\cong \frac{\mu_0 W_1 T(3N-1)g + \mu_0 W_1 TNh}{2g(g+h)} \\ G &\cong \frac{\mu_0 W_1 TNh - \mu_0 W_1 TN(N-1)g}{2g(g+h)} \\ \varphi &= \frac{2\pi}{p}x \end{aligned} \tag{2}$$

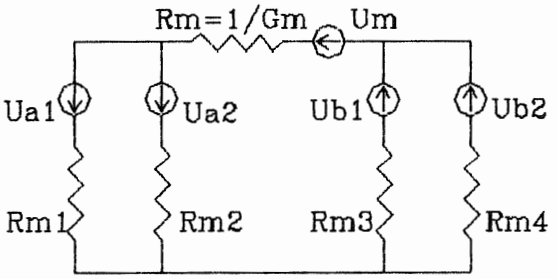

FIGURE 3: Equivalent Circuit of Actuator

Where W_1 is width of one tooth, N is number of teeth, h is height of tooth, T is thickness of pole, g is air gap length, μ_0 is magnetic permeability of vacuum, p is the period of platen tooth, x is the lateral displacement. The attractive and propulsive forces generated by the actuator are

$$F_z = \sum_{j=1}^{4} \frac{1}{2} U_j^2 \frac{dGm_j}{dg}$$
$$F_x = \sum_{j=1}^{4} \frac{1}{2} U_j^2 \frac{dGm_j}{dx} \qquad (3)$$

The equivalent MMFs Uj of the poles can be represented as follows

$$U_1 = \frac{2G_0G_m(U_{a1}+U_m)+(U_{a1}-U_{a2})G_2(2G_0+G_m)+K_2}{K_1}$$
$$U_2 = \frac{2G_0G_m(U_{a2}+U_m)+(U_{a2}-U_{a1})G_1(2G_0+G_m)+K_2}{K_1}$$
$$U_3 = \frac{2G_0G_m(U_{a3}+U_m)+(U_{a3}-U_{a4})G_4(2G_0+G_m)+K_3}{K_1}$$
$$U_4 = \frac{2G_0G_m(U_{a4}+U_m)+(U_{a4}-U_{a3})G_3(2G_0+G_m)+K_3}{K_1}$$
$$K_1 = 4G_0(G_0+G_m)$$
$$K_2 = U_{a3}G_3G_m + U_{a4}G_4G_m$$
$$K_3 = U_{a1}G_1G_m + U_{a2}G_2G_m$$

Electromagnetic Actuator Design

The design procedure starts with design requirements for the actuator including the mass of the platen and the lateral acceleration that define the attractive and propulsive forces. There are some initial characteristics such as

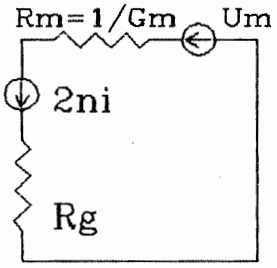

FIGURE 4: Simplified Circuit

the saturation flux density of the magnetic material, the recoil permeability of the permanent magnet material, the operating point of the permanent magnet. It is reasonable to simplify the actuator model for design procedure and then to check the calculation results using equations for actuator forces (3). The actuator is designed to satisfy the force requirements by choosing the flux densities in the air gaps and the geometrical dimensions. The initial selection of the maximal flux density and the pole cross section area sets the attractive force level of the actuator. The flux densities in any section of the magnetic bearing are limited by the saturation value of the magnetic material. In this application the flux density from the PM is greater than that from the electromagnet. The outside dimensions of the core are selected to place the operating point at nominal air gap on the linear region of the core material B-H curve. In following analysis we suppose that the mini-step drive MMFs are not applied on the coils and there is no the lateral movement of the platen. Figure 4 represents the equivalent circuit of the actuator for this case, where ni is controlled bias MMF, Rg is the magnetic reluctance of the equivalent air gap.

$$Rg = \frac{1}{Go} \qquad (4)$$

The MMF of the PM is

$$Um = BrAmRm \qquad (5)$$

Where Br is the remeance, Am is the cross section area of PM. The reluctance of PM is

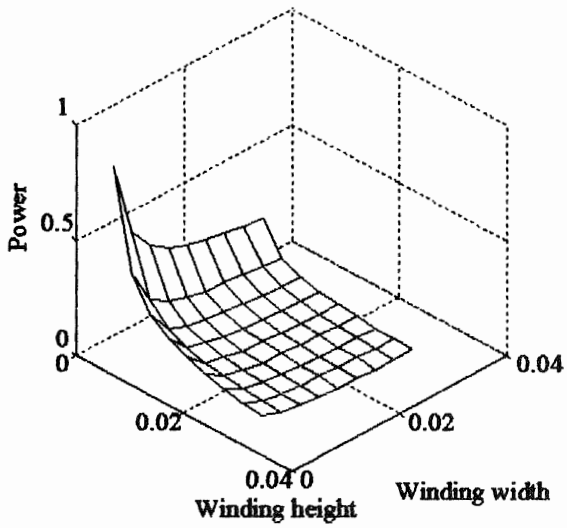

FIGURE 5: Power Surface Plot

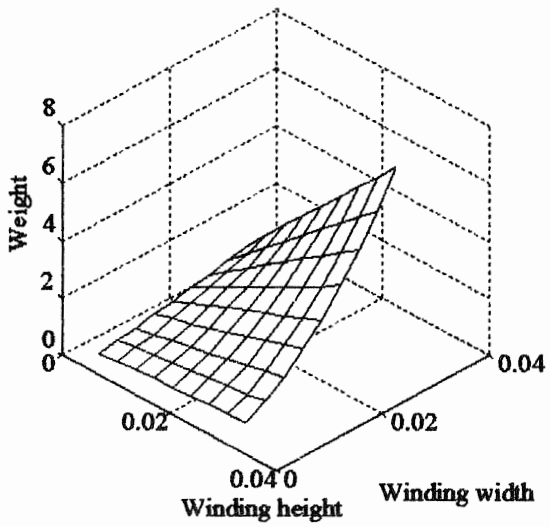

FIGURE 6: Weight Surface Plot

$$Rm = \frac{Lm}{\mu_0 \mu_r Am} \quad (6)$$

Where Lm is length, μ_r is recoil permeability of PM. For most applications the PMs operate in the second quadrant of the B-H curve. The B-H curves for the modern rare-earth magnets are nearly straight lines between the Br and the coercive force Hc. The equation of B-H curve is

$$Bm = \mu_0 \mu_r Hm + Br \quad (7)$$

Where Hm is magnetizing force of permanent magnet. The recoil permeability is the slope of the minor hysteresis loop. The minor hysteresis loop follows the B-H curve and the μ_r is the ratio of Br and Hc. Ampere's circular law for circuit can be written as

$$HmLm + BgAgRg = 2ni \quad (8)$$

Where Bg is flux density across the air gap, Ag is the cross section area. The magnetic flux equation which connects the required flux density across the air gap and the operating flux density of the magnet is

$$BmAm = BgAg \quad (9)$$

From equation (7), (8) and (9), the operating flux density of the magnet can be represented as

$$Bm = \frac{Br}{[1 + \frac{\mu_0 \mu_r AmRg}{Lm}]} + \frac{2ni}{[\frac{Lm}{\mu_0 \mu_r} + AmRg]} \quad (10)$$

The first part of the equation (10) can be treated as a constant operating flux density of the PM and can be used for permanent magnet design. The second part of the equation is the variation of the operating flux density caused by the magnetizing force from the coils and can be used for electromagnet design independently of PM design.

For maximum energy output from PM, the operating flux density should be about the half of its remanence and should be equal to assumed for PM part of the required flux density across the air gap. After that the length and cross section area of the magnet can be chosen with the help of the equation (10).

To optimize the actuator design in accordance with the required power consumption, the power and weight for various dimension ratios for given force level of the actuator can be calculated. The force level can be represented by the following simplified equation

$$F_z = \frac{2A_p B_{max}^2}{\mu_0} \tag{11}$$

Where *Bmax* is part of air gap induction induced by coils, *Ap=WT* is cross section area of air gap for one pole. *W=NW1* is width of one pole. The power dissipated in winding is

$$P = \rho \frac{B_{max}^2 g^2 l_{av}}{\mu_o k_p A_w} \tag{12}$$

Where ρ=1.7e-8 is copper resistivity, l_{av} is the average winding length, *Aw* is the winding cross section area, k_p is winding packing factor.

$$l_{av} = 2W + 2T + 4a \tag{13}$$

$$A_w = ab \tag{14}$$

a is the winding width, *b* is the winding height.

The actuator weight can be written as

$$Wht = \delta_I(4WTb + 8W^2T + 12WTa) + \delta_C(8Wab + 8Tab + 16a^2b) \tag{15}$$

δ_I=7.8e3 is iron density, δ_C=8.9e3 is copper density.

The Figures 5,6 show power and weight surface plots that correspond to following parameters of actuator: *W*=6e-3 m; *T*=18e-3 m; *g*=5e-4 m; *Bmax*=.25*Bm*=.2 Tesla. The algorithm shown can be used for choosing the appropriate width and height of winding. Then the length *L* and height *H* of actuator can be chosen in accordance with the equations

$$L = 4W + 6a$$
$$H = 2W + b \tag{16}$$

The results of actuator design that have been gotten on the basis of simplified actuator model should be checked with the help of initial model and equations (3).

CONTROL SYSTEM DESIGN

To provide the precision coordinate measurements and to achieve the platen levitation the different sensor systems were analyzed. The capacitive sensors and electronics have been designed that can provide the required nanometer resolution and adequate bandwidth.

The control system is the key element determining performance of precision magnetic bearing system. To provide low-noise control system design, the analysis of the disturbances and their mathematical models are necessary. The main disturbances in the system are mechanical vibrations (vibration's noise) of the frame and sensor noise. These disturbances are random signals. The time wave form of the noise is very complex and the exact amplitude at any time cannot be predicted. Since noise is random, we characterize it statistically. The analysis of the measured vibration acceleration signal and sensor noise showed that the signal amplitudes follow a Gaussian probability distribution with a mean of zero [3]. Therefore, we can accept that the vibration signal and sensor noise are white noises with known spectral densities which go through the first-order low-pass filters with the known noise bandwidth.

Now we can use the theory of statistical dynamics for the analysis of our control system [4]. The equations for the variance and for the peak-to-peak deviation of the output signal in dependence of the parameters of the system were developed which allow us to choose these parameters in accordance with the required peak-to-peak deviation of output signal and system's bandwidth.

CONCLUSIONS

This paper has introduced a precision motion control magnetically suspended XY stage. The equations for attractive and propulsive forces of actuators were derived and their design was optimized to maximize the power efficiency and minimize the influence of the propulsive movement on the vertical coordinate of the platen.

The experimental measurements of the vibration's acceleration in laboratory and noise of capacitive sensors, combined with the statistical approach to the design of the control system [3] and simulations of the system under closed-loop control, indicate that stage should be capable of operating to its resolution and required 50 mm travel range in two linear directions.

A hardware prototype of a precision magnetically suspended XY stage is now under construction, allowing experimental verification of the performance that has been predicted.

REFERENCES

1. Trumper D.L., Queen M.A. Precision Magnetic Suspension Linear Bearing, Symposium on Magnetic Suspension Technology, NASA LaRC, Hampton, VA, Aug. 19-23, 1991, pp.89-104.
2. Higuchi T. Magnetically Suspended Stepping Motors for Clean Room and Vacuum Environments, Proceedings of the 2nd International Symposium on Magnetic Suspension Technology, Seattle, Washington, Aug. 11-13, 1993, p.11b-1.
3. Kuzin A.V., Holmes M.L., Behrouzjou R., Trumper D.L. Analysis of Achievable Disturbance Attenuation in Precision Magnetically-Suspended Motion Control System, Proceedings of the 2nd International Symposium on Magnetic Suspension Technology, Seattle, Washington, Aug. 11-13, 1993, p.11b-19.
4. Kuzin A.V., Holmes M.L., Trumper D.L. Analysis and Design of the Control System for a Precision Magnetically-Suspended Six-Degree-of-Freedom Motion Control Stage, Proceedings of MAG 93 International Conference and Exhibition, July 1993, Alexandria, VA USA, pp.65-73